Arrester Bed

Lucas Hinsching Mostafá, Brazil, lucasmostafa@gmail.com

ARTICLE INFO

Participated in IYPT 2023

Awarded by Ariaian Young Innovative Minds Institute , AYIMI

http://www.ayimi.org ,info@ayimi.org

ABSTRACT

A sand-filled lane results in the dissipation of the kinetic energy of a moving vehicle. What length is necessary for such an arrester bed to entirely stop a passively moving object (e.g. a ball)? What parameters does the length depend on? To study this phenomenon several experiments have been done and the results are compared with theory to find the best situation in reality.

Keywords : *: Moving vehicle, arrester bed, length, parameters*

1. Introduction

The arrester bed is used in roads to decelerate cars or trucks that lost control. Some studies were made so that this deceleration would be maximized, and accidents minimized, therefore, what the problem proposes is an analysis of this behavior.

For the model used in the following, we considered the object to be either a cylinder or a sphere. As seen in some preliminary observations and that can also be concluded intuitively, the main analysis should be the relationship between the sand and the object parameters.

2. Theory

2.1. Cylinder's Coordinates and Properties

For the phenomenon there are two main forces that lead the motion, the shear stress $(\vec{\tau})$ and the normal tension $(\vec{\sigma})$ which are the rolling friction and the normal for the interaction between objects and granular soils (Fig. 1).

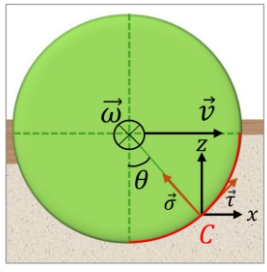

Fig. 1: Diagram of forces (shear stress and normal tension)

Other important parameters are the angular velocity $(\vec{\omega})$, linear velocity $(\vec{v})$, Coordinates *X, Z* and θ, as well as the contact surface C (Fig. 2).

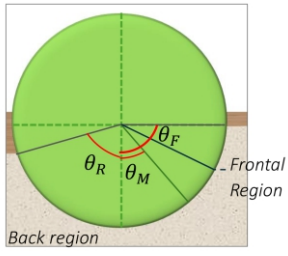

Fig. 2: Definition of frontal and back region and maximum theta

As we defined theta, some specific values will be important, such as the ones of initial (θ_F) and final contact (θ_R) with the sand, and one in which the normal tension is maximum (θ_M).

After defining the latter thetas it is possible to describe the sinking depth *(Z)* as a function of them(Eq. 1).

$$\theta_M \leq \theta \leq \theta_F\colon\ z = R(\cos(\theta) - \cos(\theta_F)) \tag{1}$$

To get to a motion equation it is better to separate them in the *Z* and *X* axis, which can be done decomposing the normal tension and the shear stress as the equation (2).

$$\overrightarrow{\sigma_z} = (\sigma\, cos(\theta) + \tau\, sin(\theta))\hat{z} \tag{2}$$

As said, now it becomes possible to achieve the motion equations by integrating the resultant of them $(\overrightarrow{\sigma_T} = \overrightarrow{\sigma_z} + \overrightarrow{\sigma_x})$ all over the contact surface C (Eq. 3).

$$\begin{pmatrix} F_x \\ F_z \end{pmatrix} = \int_C \overrightarrow{\sigma_T}, \hat{n}\, bR\, d\theta \tag{3}$$

With *b* being the cylinder width and *R* the radius. Separating the forces at *X* and *Z* and using the definition of torque the three equations of motions are found (Eqs. 4-6).

$$m\ddot{x} = \int_C (\tau\, cos(\theta) - \sigma\, sin(\theta)\, Rb)d\theta \tag{4}$$

$$m\ddot{z} = \int_C (\sigma\, cos(\theta) + \tau\, sin(\theta)\, Rb)d\theta - mg \tag{5}$$

$$I\dot{\omega} = \int_C R\tau(\theta)Rbd\theta \tag{6}$$

2.2. Pressure Model and Distribution

During the preliminary observations it was possible to observe a relevant dependence on the sand properties, and to find the normal tension and the shear stress, we chose the model of Beker.

This model was proposed in such a way that the pressure exerted by a flat surface on a granular soil would be proportional to the sinking depth multiplied by factors that include both the sand and the surface properties described in the following equation (Eq. 7).

$$\sigma = \left(ck_c + \rho k_\phi \mathrm{b}\right)\left(\frac{\mathrm{z}}{\mathrm{b}}\right)^{\mathrm{n}} \tag{7}$$

In which σ is the normal tension, *c* is the tension of ground cohesion; is the sand density ρ and k_c are the constants for

a single combination of a granular soil and a flat surface that can be found experimentally; b is the cylinder width; z is the sinking depth and n is the sinking exponent.

The tension of ground cohesion is a parameter that measures how strong is the interaction between the particles of sand, which is assumed to be 0 for dry sand, yielding in a n between 0.5 and 2.0.

Using the equation of the Beker model with the expression of the sinking depth found before we get an expression for σ_1 which is the normal tension at the frontal region (Eq. 8) $(\theta_m < \theta < \theta_f)$.

$$\sigma_1 = (\rho k_\phi b)\left(\frac{R}{b}\right)^n (\cos(\theta) - \cos(\theta_f))^n \quad (8)$$

As shown in the figure (3), there is a pressure distribution that follows a mountain shape on the cylinder, therefore a simetry between the frontal and back region can be stablished around the point of maximum normal tension.

Mathematically we can find a theta from $\theta_M < \theta < \theta_R$ that is equivalent to another one in $\theta_m < \theta < \theta_f$ and get the other values of normal tension as follows (Eq. 9).

$$\sigma_2 = (\rho k_\phi b)\left(\frac{R}{b}\right)^n \left(\cos\left(\theta_F - (\theta_F - \theta_M)\frac{\theta}{\theta_M}\right) - \cos(\theta_f)\right)^n \quad (9)$$

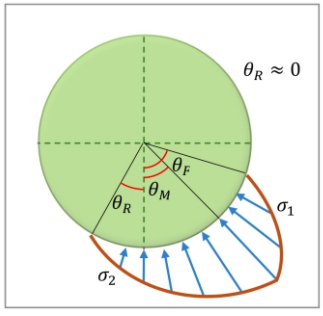

Fig. 3: Diagram of pressure distribution (blue arrows)

2.2.1 Shear Stress

Similarly to the rolling friction, for the cylinder to roll there must be friction and thus, it dependent on the normal, or in this case, the normal tension.

For that some parameters were added, such as the parameter of shear deformation (k) and the angle of ground friction (ϕ), which are found experimentally and vary from soil to soil, and the last one, the distance of ground displacement j, as observed, some particles of sand are pushed backwards due to the rolling motion of the cylinder, and j is the distance traveled by these particles. However, as stated before, one of our considerations is that the sand is dry and therefore c is negligible . So the equation becomes(Eqs. 10-11).

$$\tau(\theta) = (c + \sigma(\theta)\tan\phi)(1 - e^{-j/K}) \quad (10)$$

$$\tau(\theta) \approx (\sigma(\theta)\tan\phi)\left(1 - e^{-j/K}\right) \quad (11)$$

To calculate j we define it throughout the slipping speed which is given by $v_s = \omega R - \dot{x}\cos\theta$ achieving the integral form (Eqs. 12-13).

$$j = \int_\theta^{\theta_F} (\omega R - \dot{x}\cos\theta)\frac{d\theta}{\omega} \quad (12)$$

$$j = R(\theta_F - \theta) - \frac{\dot{x}}{\omega}(\sin(\theta_F) - \sin(\theta)) \quad (13)$$

2.2.2. Angle of Maximum Pressure

As the shear stress has two defined regimes which depend on the angle theta it must be defined, that is what we will explore a little bit.

For that we used a paper by Jo-Woung Wong and A.R. Reece as a reference. The equation that will describe the behavior of the angle of maximum normal tension is as equation (14).

$$\theta_m = \left(a_1 + a_2\frac{b}{R}\right)\theta_f \quad (14)$$

which the effect of the ratio b/R gets clearer with the following diagrams (Figs 4a,b and c).

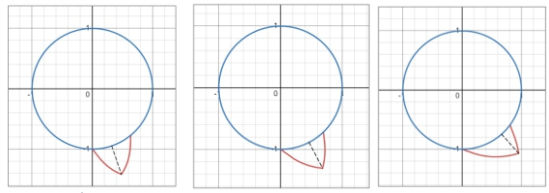

(a) (b) (c)

Fig. 4: a) b/R=0.5; b) b/R=1.5 ; c) b/R=2.5

Therefore as the ratio gets greater the angle increases and therefore is closer and closer to the horizontal axis, leading to a greater resistance force. It is important to notice that the parameters a_1 and a_2 fixed values for the material used in the cylinders:

$$a_1 = (0.30 \pm 0.04); a_2 = (0.15 \pm 0.01)$$

2.3. Motion Equations

As all the normal tension and the shear stress which were unknown before are now explained and found mathematically, we can return to the initial equations for $\ddot{x}, \ddot{z}$ and $\ddot{\theta}$ to substitute σ and τ to get a complete solution of the phenomenon.

The equations for the x, z and θ coordinates then become(Eqs. 15-17).

$$m\ddot{x} = Rb\int_C \sigma(\theta)\left(-A_1(\theta) - B_1(\theta)e^{-\frac{\dot{x}}{\omega K}(\sin(\theta)-\sin(\theta_f))}\right)d\theta \quad (15)$$

$$m\ddot{z} = \int_C \sigma(\theta)\left\{A_2(\theta) + B_2(\theta)e^{\frac{\dot{x}}{\omega K}(\sin(\theta)-\sin(\theta_f))}\right\}d\theta - mg \quad (16)$$

$$I\dot{\omega} = R^2 b\int_C \sigma(\theta)\left[A_3(\theta) - B_3(\theta)e^{\frac{\dot{x}}{\omega K}[\sin(\theta)-\sin(\theta_f)]}\right]d\theta \quad (17)$$

In which the coefficients A_ and B_ were used to shorten the solution. An interesting thing that can be observed with mathematical development is that the integral in the mg really fast, therefore the cylinder achieves a constant sinking depth in the soil surface from the fact that the resultant force in z is nude in most of the motion.

2.4. Parameter calculation k_ϕ

This parameter relates the amount of contribution that the density and the size parameter of the cylinder will contribute to the normal tension exerted on the object.

This can be made by linearizing the equation for pressure using logarithm (Eq. 18).

$$\log(\sigma) = \log(\rho k_\phi b) + n\log\left(\frac{z}{b}\right) \quad (18)$$

By plotting the linearized form of the equation the graph

is found, and by comparing the fit values with the coefficients we find the value of n and ρk_ϕ (Fig. 5).

$$n = (1{,}38 \pm 0{,}03) \qquad \rho k_\phi = (10{,}4 \pm 0{,}32)Pa$$

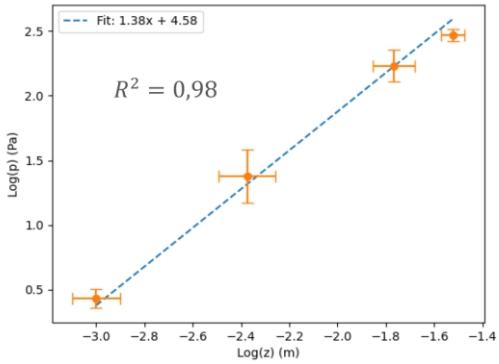

Fig. 5: Linearized graph of pressure

3. Experimental Setup

In the experimental setup the following materials were used:

- Cylinders made of ABS of different dimensions, some only changed height, others, width
- Ramp made of MDF for launch, which was standardized by using tweezers.
- Acrylic box of dimensions 50* 10 * 5 cm^3
- Different types of sand, such as natural quartz and dolomite, in which some only the density changed (black basalt and dolomite) and other only the size change, e.g. dolomite.
- Cellphone camera
- Ruler

4. Results

The analysis of the data taken using tracker and comparing to the predicted behavior of the equations of motion found theoretically leads to some interesting conclusions regarding the influence of some parameters.

The first one was the cylinder mass, in which we maintained the geometrical proportions constant, but changed the material. It can be thought that the change of the material would yield in a change of friction and therefore interfere in the system, it showed to be a false statement, since the properties of the sand have a much greater relevance on the phenomenon.

As seen, if the mass increases the distance traveled by the objects decreases, since the more massive the objects gets the greater the resistive forces get, because it is sinking more in the soil. Note that the continuous line is a theoretical plot and the points are experimental data with the respective error bars.

Another analysis made was of the diameter of the cylinder, which was changed with easily since the cylinder were made on a 3D printer. From the graph, it is possible to assert that as the diameter is bigger, also is the resistance forces, since an increase in the diameter leads to an increase in the shear tensor.

Finally, the last parameter we can vary of the cylinder is the height *b*. This variation would lead to an increase in the area of contact between the soil and the object and thus, increase the resistance forces and the displacement will decrease (Figs. 6-8).

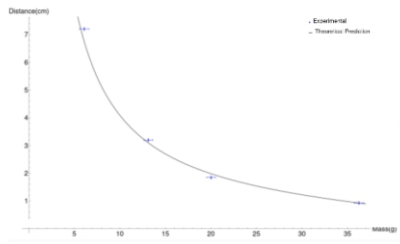

Fig. 6: Graph of Distance per mass; experimental and theoretical comparison

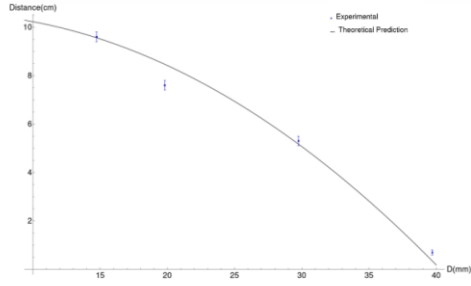

Fig. 7: Graph of Distance per Diameter; experimental and theoretical comparison

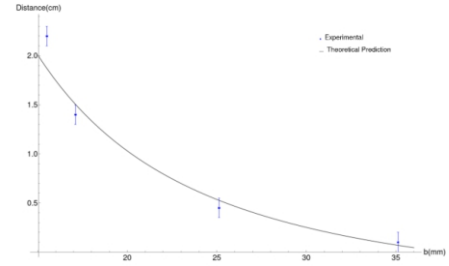

Fig. 8: Graph of Distance per Cylinder height; experimental and theoretical comparison

Another possible analysis due to the experimental setup is the variation of the density of the particles of sand. As can be observed, as the density increases the displacement decreases, but the most interesting is that some points have a huge deviation from the theoretical predication, which comes from the fact that these particles of sand are too big (between 3.00 to 5.00 mm for the most deviated point). Therefore our theory only holds for certain sizes of particle, and the behavior of a granular soil does not maintain for great values (Fig. 9).

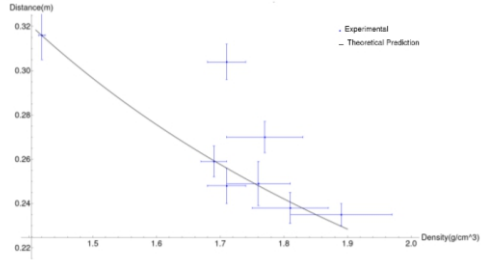

Fig. 9: Graph of Distance per Soil Density'; experimental and theoretical comparison

To check on the validity of our theory with another approach, we compared the prediction of the loss of kinetic energy with the experimental data, as it was one of the topics the problem statement stood up (Fig. 10).

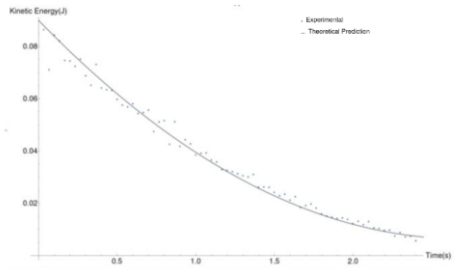

Fig. 10: Graph of the Kinetic energy per time; theoretical and experimental comparison

As said before, another possible object to analyze this situation is the sphere, and so we compared experimentally what would happen for this geometry. From the data we can see that the cylinder presences a resistance force greater than the sphere does, and so the latter has a longer displacement.

5. Conclusion

This work presented an analysis of the behavior of the arrester beds that can be seen on the roads and help prevent accidents due to its deceleration characteristics. For the theoretical approach we used a model of tensors and found equations for the axis we defined. For later development we made some experiments and took data so that it was possible to compare the theoretical predictions with the real data (Fig. 11).

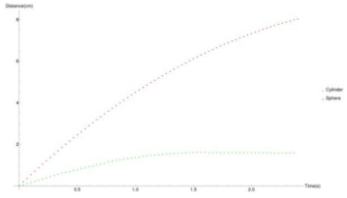

Fig. 11: Graph of a experimental comparison between the displacement of a cylinder and a sphere

Therefore we explored both the parameters of the cylinder and of the granular soil that would affect the displacement of the object during the phenomenon.

References

[1] Coutermarsh, B. (2007). Velocity effect of vehicle rolling resistance in sand. Journal of Terramechanics, 44(4), 275–291.

[2] De Blasio, F.V., Saeter, M.B.: Rolling friction on a granular medium. Phys. Rev. E 79, 022301 (2009)